



Design and Calibration of an Airborne Multichannel Swept-Tuned Spectrum Analyzer

*Philip J. Hamory
Dryden Flight Research Center
Edwards, California*

*John K. Diamond
Langley Research Center
Hampton, Virginia*

*Arild Bertelrud
Analytical Services and Materials, Inc.
Edwards, California*

The NASA STI Program Office...in Profile

Since its founding, NASA has been dedicated to the advancement of aeronautics and space science. The NASA Scientific and Technical Information (STI) Program Office plays a key part in helping NASA maintain this important role.

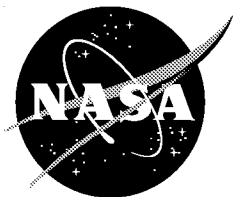
The NASA STI Program Office is operated by Langley Research Center, the lead center for NASA's scientific and technical information. The NASA STI Program Office provides access to the NASA STI Database, the largest collection of aeronautical and space science STI in the world. The Program Office is also NASA's institutional mechanism for disseminating the results of its research and development activities. These results are published by NASA in the NASA STI Report Series, which includes the following report types:

- **TECHNICAL PUBLICATION.** Reports of completed research or a major significant phase of research that present the results of NASA programs and include extensive data or theoretical analysis. Includes compilations of significant scientific and technical data and information deemed to be of continuing reference value. NASA's counterpart of peer-reviewed formal professional papers but has less stringent limitations on manuscript length and extent of graphic presentations.
- **TECHNICAL MEMORANDUM.** Scientific and technical findings that are preliminary or of specialized interest, e.g., quick release reports, working papers, and bibliographies that contain minimal annotation. Does not contain extensive analysis.
- **CONTRACTOR REPORT.** Scientific and technical findings by NASA-sponsored contractors and grantees.
- **CONFERENCE PUBLICATION.** Collected papers from scientific and technical conferences, symposia, seminars, or other meetings sponsored or cosponsored by NASA.
- **SPECIAL PUBLICATION.** Scientific, technical, or historical information from NASA programs, projects, and mission, often concerned with subjects having substantial public interest.
- **TECHNICAL TRANSLATION.** English-language translations of foreign scientific and technical material pertinent to NASA's mission.

Specialized services that complement the STI Program Office's diverse offerings include creating custom thesauri, building customized databases, organizing and publishing research results...even providing videos.

For more information about the NASA STI Program Office, see the following:

- Access the NASA STI Program Home Page at <http://www.sti.nasa.gov>
- E-mail your question via the Internet to help@sti.nasa.gov
- Fax your question to the NASA Access Help Desk at (301) 621-0134
- Telephone the NASA Access Help Desk at (301) 621-0390
- Write to:
NASA Access Help Desk
NASA Center for AeroSpace Information
7121 Standard Drive
Hanover, MD 21076-1320



Design and Calibration of an Airborne Multichannel Swept-Tuned Spectrum Analyzer

*Philip J. Hamory
Dryden Flight Research Center
Edwards, California*

*John K. Diamond
Langley Research Center
Hampton, Virginia*

*Arild Bertelrud
Analytical Services and Materials, Inc.
Edwards, California*

National Aeronautics and
Space Administration

Dryden Flight Research Center
Edwards, California 93523-0273

NOTICE

Use of trade names or names of manufacturers in this document does not constitute an official endorsement of such products or manufacturers, either expressed or implied, by the National Aeronautics and Space Administration.

Available from the following:

NASA Center for AeroSpace Information (CASI)
7121 Standard Drive
Hanover, MD 21076-1320
(301) 621-0390

National Technical Information Service (NTIS)
5285 Port Royal Road
Springfield, VA 22161-2171
(703) 487-4650

DESIGN AND CALIBRATION OF AN AIRBORNE MULTICHANNEL SWEPT-TUNED SPECTRUM ANALYZER

Philip J. Hamory

**National Aeronautics and Space Administration
Dryden Flight Research Center
Edwards, California**

John K. Diamond

**National Aeronautics and Space Administration
Langley Research Center
Hampton, Virginia**

Arild Bertelrud

**Analytical Services and Materials, Inc.
Edwards, California**

ABSTRACT

This paper describes the design and calibration of a four-channel, airborne, swept-tuned spectrum analyzer used in two hypersonic flight experiments for characterizing dynamic data up to 25 kHz. Built mainly from commercially available analog function modules, the analyzer proved useful for an application with limited telemetry bandwidth, physical weight and volume, and electrical power. The authors discuss considerations that affect the frequency and amplitude calibrations, limitations of the design, and example flight data.

KEY WORDS

Spectrum analysis, Signal processing, Multiple input calibration, Multivariable calibration, Analog circuits

INTRODUCTION

In 1994 and 1998 NASA flew two hypersonic aerodynamic experiments called FX-A and FX-1, respectively, aboard the Pegasus^{®*} launch vehicle as part of a project called PHYSX (for Pegasus[®] HYperSonic eXperiments) (ref. 1). The requirements for these experiments included dynamic data up to 25 kHz to characterize the vibration environment and the state of the boundary layer. Real-time transmission of time histories of the dynamic data via a pulse code modulation telemetry encoder would require sample rates of at least 50,000 samples per second (sps). The telemetry bandwidth necessary to support those sample rates was not available, so two airborne spectrum analyzers were developed: one based on the swept-tuned receiver, and one based on digital signal processing (DSP) technology. The frequency content of the data was of most interest, and transforming the data into the frequency domain with an onboard spectrum analyzer offered the opportunity to trade off frequency resolution for a reduced bandwidth.

Work on developing the DSP-based analyzer has been reported previously (refs. 2 and 3), but work on the swept-tuned analyzer has not yet been reported. (The design of a related analyzer was reported in ref. 4.) This paper describes the design and calibration of the swept-tuned analyzer used on FX-A and FX-1. The design discussion includes the underlying signal processing technique, the circuit elements, packaging, and limitations. A calculation showing the tradeoff between frequency resolution and telemetry bandwidth is also presented. The calibration discussion includes the process and considerations that affect the frequency and amplitude calibration coefficients. Finally, FX-A flight data are presented to show results obtained from actual flight conditions. Use of trade names or names of manufacturers in this document does not constitute an official endorsement of such products or manufacturers, either expressed or implied, by the National Aeronautics and Space Administration.

DESIGN

Introduction to the Design

The fundamental technique used in this design is the same as that of laboratory spectrum analyzers. Reference 5 is an excellent presentation on spectrum analysis basics, and the discussion in this paper is organized and written based upon that presentation. Reference 6 also contains a section (ref. 6(a)) on the subject.

Spectrum analyzers are typically used for radio frequency (RF) measurements. Because the required measurement bandwidth for FX-A and FX-1 extended only slightly beyond the audio range, commercially available analog function modules were used rather than RF components.

Another difference between this analyzer and a laboratory spectrum analyzer is that this analyzer has no display unit. Rather, an airborne telemetry encoder samples its amplitude and frequency analog outputs. By plotting the amplitude readings against the frequency readings, engineers on the ground obtain the display of data. Calibrations are applied digitally on the ground.

*Pegasus[®] is a registered trademark of Orbital Sciences Corporation, Fairfield, Virginia.

The Design Elements

A spectrum is a range of frequencies, and a spectrum analyzer is a device that breaks up a signal into its frequency components. The most common type of spectrum analyzer is the swept-tuned receiver, the most widely accepted, general-purpose tool for frequency domain measurements. The technique most widely used is superheterodyne. Heterodyne means to mix—that is, to translate frequency—and super refers to frequencies above the audio range. Basically, these analyzers use a bandpass filter as a window to view a limited part of the signal's spectrum, and this window appears to sweep across the spectrum and identify all the frequency components present.

It is difficult, however, to build a filter that tunes over a wide range. An easier implementation is to use a tunable local oscillator (LO) and keep the bandpass filter fixed. In this implementation, the input signal sweeps past the fixed filter. For now, assume that this resembles how an AM radio works except that a radio dial controls the tuning and the radio has a speaker instead of a display. The concept will become more clear later in this paper's discussion of the circuit elements of the analyzer.

The major components in this spectrum analyzer, as figure 1 shows, are the input filter, analog multiplier, intermediate frequency (IF) filter, root-mean-square (RMS) to direct current (DC) converter, local oscillator, and sweep generator. The analog multiplier, IF filter, RMS-to-DC converter, and voltage-to-frequency converter in the local oscillator are the analog function modules referred to earlier. Before discussing how the components work together, this paper describes the fundamentals of each one individually.

The **analog multiplier** (ref. 7) plays the same role as the mixer in an RF spectrum analyzer; that is, it converts a signal from one frequency to another. From modulation theory, it is known that when two signals are multiplied together, the product contains frequencies that are the sum and difference of the two

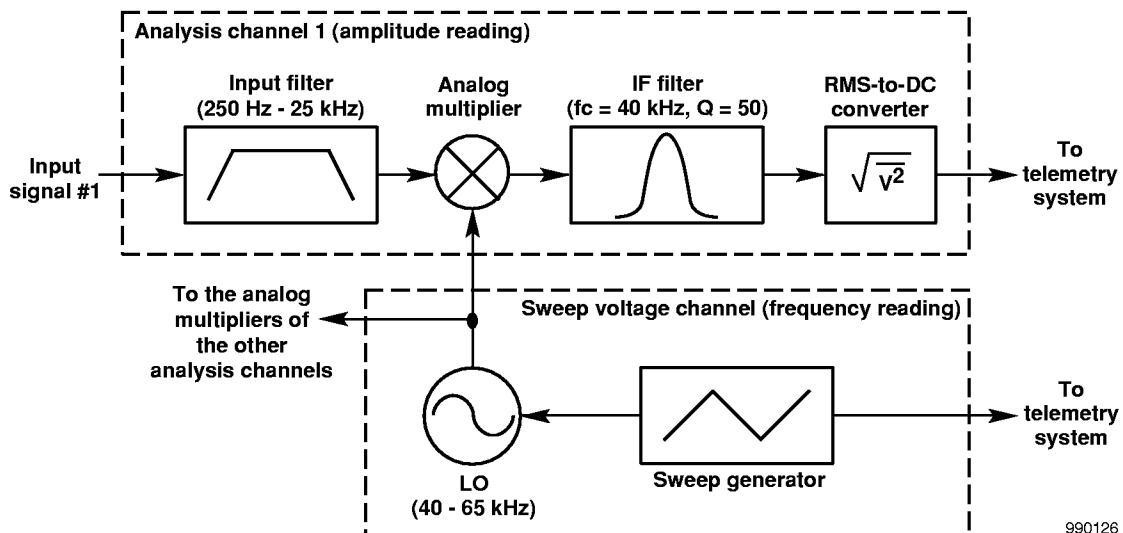


Figure 1. PHYSX swept-tuned spectrum analyzer (only one of four analysis channels shown; frequencies shown are for FX-1).

signals. The following trigonometric identity, involving frequencies F_1 and F_2 , and time t , provides a glimpse into that fact:

$$\cos(2\pi F_1 t) \cos(2\pi F_2 t) = 0.5 \{ \cos(2\pi [F_1 + F_2] t) + \cos(2\pi [F_1 - F_2] t) \} \quad (1)$$

In this spectrum analyzer, the difference frequency is of interest. The multiplier has converted the input signal to an IF that the analyzer can now detect.

The **IF filter** is a narrow bandpass filter used as the window for detecting signals. In this design, eight second-order analog filter stages (ref. 8) are cascaded together. Each stage is identical, having a center frequency (f_c) of 40 kHz and a quality factor (Q) of 15. The entire filter has a total Q of 50 yielding a resolution bandwidth of 800 Hz.

The analyzer must convert the IF signal to a baseband signal that the telemetry encoder can sample. This is accomplished with an envelope detector. The output of the narrow bandpass filter is AC coupled to the detector, and the output from this detector represents the amplitude of the spectrum. An **RMS-to-DC converter** (ref. 9) was selected as the detector because detecting the power of the signal was of interest. In general, a true power measurement can be made only by averaging the square of the actual voltage waveform (ref. 6(b)). Although the RMS-to-DC converter actually gives the square root of the true power, the square root was accepted to benefit from the quality and compactness of the commercially available converter. The averaging time of the RMS-to-DC converter was set to the minimum time described in reference 9. For FX-1, this time was 12.5 microseconds (μs).

The **local oscillator** is the element that, in effect, tunes the analyzer, and this element was constructed out of three parts: a voltage-to-frequency converter, a digital sine-wave generator, and a bandpass filter.

A sine-wave generator can be constructed out of digital circuitry by hooking up a shift register as a walking-ring counter and by resistively summing the register outputs to produce a staircase waveform. When passed through a bandpass filter to remove the DC component and high-order frequency components, the staircase waveform produces a low-distortion (less than 1 percent), sinusoidal output with stable amplitude. For this application, a 5-stage shift register was used to make a 10-stage walking-ring counter (ref. 10). A voltage-to-frequency converter (ref. 11) drove the counter's clock and was in turn driven by the sweep generator.

The **sweep generator** is a precision, temperature-stable, triangle waveform generator (ref. 12) that tunes the LO to change its frequency linearly. The telemetry encoder samples this voltage and the results represent the frequency component of the signal being analyzed. Most swept-tuned spectrum analyzers use a ramp generator and, therefore, sweep across the spectrum unidirectionally. Even though a bidirectional sweep makes the calibration process more involved, the triangle wave was chosen for circuit simplicity.

The **input filter** is a wideband anti-aliasing filter. The filter consists of a third-order Chebyshev high-pass filter with a frequency passband beginning at 250 Hz in series with a fourth-order Chebyshev low-pass filter with a frequency passband ending at 25 kHz. Voltage-controlled, voltage-source (VCVS) hardware implementation was used for these filters. Reference 6(c) has a suitable procedure for designing equal-component VCVS filters; however, the unity-gain VCVS filter was chosen primarily because it has fewer components. Component values were computed using filter design software developed in house. Figure 2, obtained by circuit simulation, shows the nominal frequency response of the input filter.

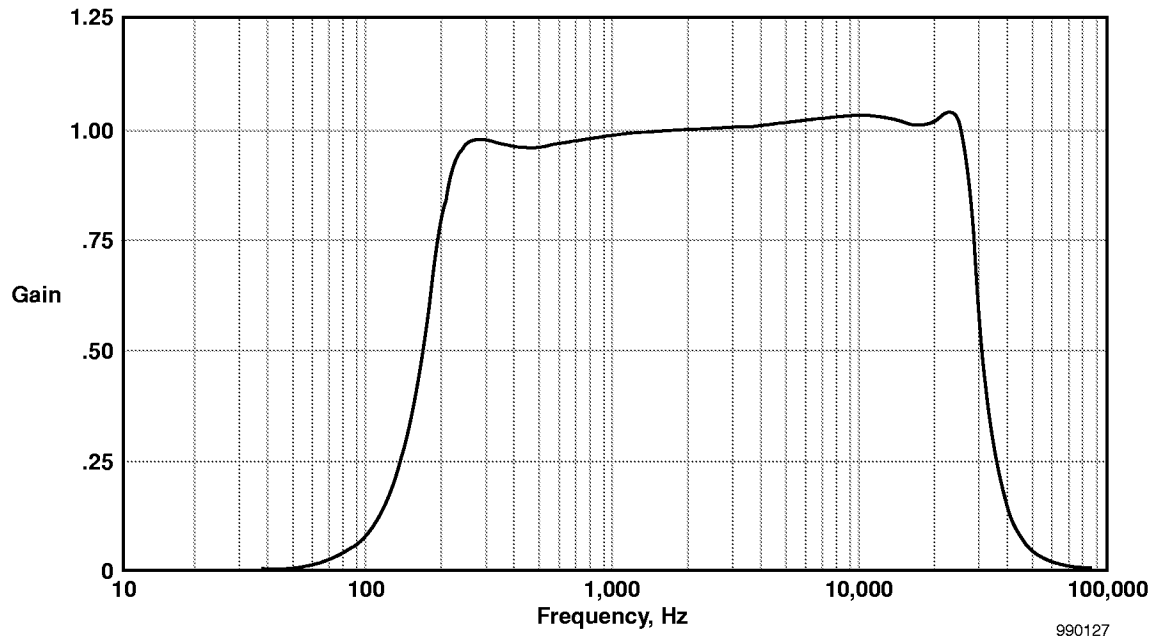


Figure 2. Nominal frequency response of input filter.

How It All Works Together

Suppose a sine-wave, whose amplitude is 1.2 V peak-to-peak (Vpp) and whose frequency f_{sig} is 10 kHz, is applied to the input. Suppose also that the telemetry system is set up to sample the analysis channel and the sweep voltage channel at the same rate. Figure 3 simulates what the calibrated output of the analyzer would look like if the points in the spectrum were 62.5 Hz apart. To visualize how this figure is constructed, imagine the sweep generator increasing in voltage causing the LO frequency (f_{LO}) to sweep upward. As soon as the difference frequency $f_{LO} - f_{sig}$ comes into the skirt of the IF filter, the signal starts to appear at the output. When the difference frequency is at the center frequency (40 kHz), the full amplitude of the signal passes through. As the sweep generator increases voltage further, the difference frequency leaves the filter skirt, and the amplitude reading goes to zero.

A swept-tuned analyzer only produces a correct spectrum when the sweep rate is fast enough to capture the spectrum before it changes. On the other hand, the response time of the IF filter (about 1 millisecond (ms) in this design) limits how high the sweep rate can go. Swept-tuned analyzers are, therefore, more suited for signals whose frequency content is stationary rather than transient during the sweep time. For more details on this issue, see references 5 and 6(a).

Suppose the period of the sweep generator triangle wave is 200 ms (as it was in this application) so that each sweep is completed in 100 ms. This arrangement gives a sweep rate of 25 kHz/100 ms or 250 Hz/ms. To acquire points that are 62.5 Hz apart, samples are needed every 250 μ s, which corresponds to 4000 sps. Therefore, to acquire data from the four analysis channels and the sweep voltage channel, the aggregate sample rate needs to be 20 ksp. In contrast, if the time history data are transmitted and the spectrum is computed digitally, a sample rate of at least 50 ksp is needed to have frequency content up to 25 kHz.

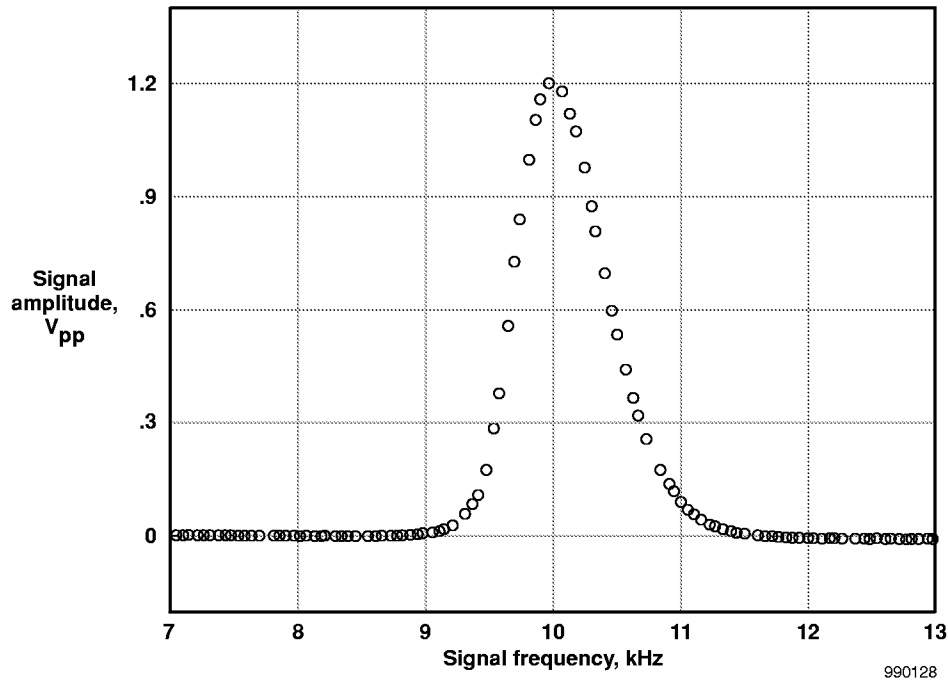


Figure 3. Simulated spectrum for 1.2 Vpp, 10 kHz sine wave (upsweep only).

For four input signals, the aggregate sample rate is 200 kps. Using the sweep time (100 ms) for the record length of a discrete Fourier transform on the time history data, the frequency resolution equals the sample rate (50 kps) divided by the number of samples in the record (5000 samples), that is, 10 Hz (ref. 13). Thus, in this example, a factor of 6.25 in frequency resolution is lost, but a factor of 10 in required telemetry system bandwidth is saved by using the airborne spectrum analyzer.

Packaging

The sweep generator and LO were placed on one circuit board measuring 6 in. \times 3.75 in. \times 0.5 in. (the last dimension includes part height), and the four analysis channels were placed on a second circuit board of the same size to make a four-channel spectrum analyzer whose total power consumption was 5.4 Watts (W) and whose weight was 0.43 lb without the chassis or 2.5 lb with the chassis. The small size, weight, and power consumption enabled the analyzer to be incorporated in experiments aboard the Pegasus® launch vehicle.

CALIBRATION

Frequency Calibration Considerations

As discussed earlier, the sweep-generator voltage determines the signal frequency that passes through the IF filters. Although one set of calibration coefficients for the sweep voltage would appear to apply to all

four input signals, this is not the case. The analysis channels have nonnegligible and unequal propagation delays. Different coefficients, therefore, apply to the sweep voltage for each input signal. Sweep direction also matters, as can be seen more clearly by studying figure 4.

Figure 4 depicts the triangular sweep voltage in the time domain. Let V_{sw_0} be the sweep voltage that causes frequency F_0 to pass through the IF filters. Let t_0 and t_0' be the times that V_{sw_0} is reached during the upsweep and downsweep, respectively. If t_{pd_1} is the propagation delay through analysis channel 1, then the amplitude readings for channel 1 are available at times $t_1 = t_0 + t_{pd_1}$ for the upsweep and $t_1' = t_0' + t_{pd_1}$ for the downsweep. If the amplitude readings and the sweep voltage are sampled at those times, then voltages V_{sw_1} and V_{sw_1}' rather than V_{sw_0} become associated with F_0 . Likewise, if the propagation delays through the other analysis channels are not equal to t_{pd_1} , as was the case in this implementation, then each analysis channel has different sweep voltages that become associated with F_0 . Thus a total of eight sets of coefficients (two sets per channel) are required to determine frequency in this four-channel analyzer.

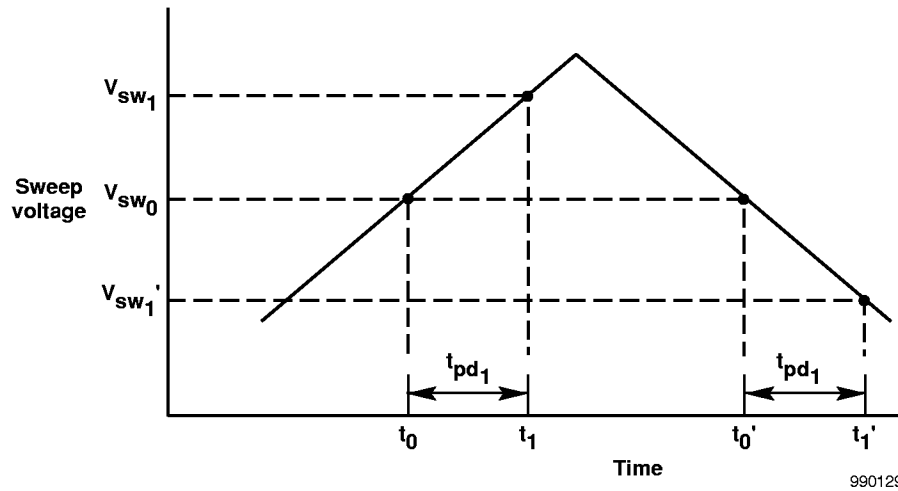


Figure 4. Sweep voltage as a function of time.

For a given channel and sweep direction, the relationship between input signal frequency and sweep voltage was linear. If the variable f represents the sweep-voltage reading, that is the frequency reading, then equation 2 can be written as follows:

$$F = p_0 + p_1 f \quad (2)$$

where p_0 and p_1 are the calibration coefficients.

Amplitude Calibration Considerations

Taking another look at figure 2, the reader will notice that the passband gain is not flat but sloped. In fact, in this implementation, the slope was greater than shown because of a limited selection of component

values and tolerances. This slope made the amplitude calibration more involved. Had the passband gain been flat, the calibration probably would have been given by equation 3,

$$V = a_0 + a_1 v \quad (3)$$

where V is the signal voltage in volts RMS, v is the amplitude reading in counts, and a_0 and a_1 are constants. Because it is not flat, the gain coefficient a_1 is a function of frequency. In figure 2, a_1 increases with frequency except for the upper transition region where a_1 decreases as frequency increases. To characterize a_1 over the entire range requires an equation that has both the frequency reading f and the inverse of the frequency reading f^{-1} . By trial and error it was found that equation 4 produced the best fit for the calibration points used.

$$a_1 = b_0 + b_1 f^{-1} + b_2 f^{-2} + b_3 f + b_4 f^2 \quad (4)$$

The overall fit was improved by letting a_0 be a function of frequency as well. See equation 5.

$$a_0 = c_0 + c_1 f^{-1} + c_2 f + c_3 f^2 + c_4 f^3 \quad (5)$$

Combining equations 3, 4, and 5, equation 6 results.

$$V = c_0 + c_1 f^{-1} + c_2 f + c_3 f^2 + c_4 f^3 + b_0 v + b_1 v f^{-1} + b_2 v f^{-2} + b_3 v f + b_4 v f^2 \quad (6)$$

Here, too, sweep direction effects required different coefficients for the upsweep than for the downsweep.

Calibration Process and Results

The analyzer inputs had a range of 0 to 1.6 Vpp from 250 Hz to 25 kHz. The analyzer was calibrated with 24 sine waves defined from a combination of 4 voltages and 6 frequencies. The sine waves were produced by a function generator that was connected to all four inputs simultaneously. For each sine wave the telemetry stream was recorded and the readings separated by sweep direction. Then, for each channel and sweep direction, the sine-wave voltage V and the frequency F was associated with the peak amplitude reading v_p and the corresponding sweep voltage reading f_p . (See figure 3 again to observe how the spectrum has a distinct peak that can be related to the input signal voltage and frequency.)

To get an accurate peak reading, data were recorded for many seconds. Because the sweep generator was asynchronous to the telemetry system, each sweep produced additional points that filled in the spectrum. The input voltage and frequency pair $\{V, F\}$ and output amplitude and frequency reading pair $\{v_p, f_p\}$ can be referred to as a calibration point. The 24 sine waves therefore produced 24 calibration points. The four voltages used were 0.4, 0.8, 1.2, and 1.6 Vpp. The six frequencies were 1, 5, 10, 15, 20, and 24 kHz.

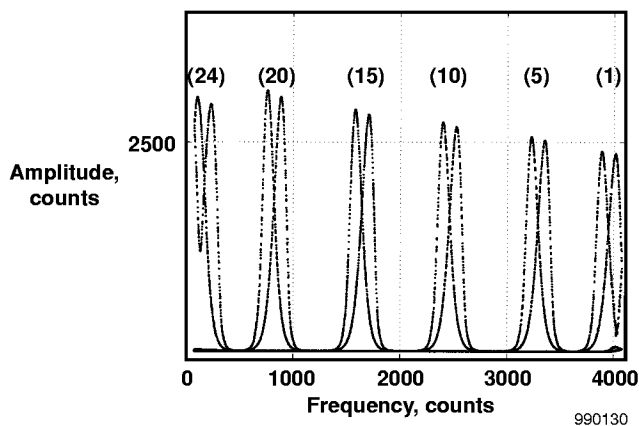
Six other calibration points were desired as well; namely, zero volts at the same six frequencies. To obtain these points, the signal inputs were grounded and the amplitude readings recorded. Because the resulting spectrum was flat, no f_p could be obtained directly. The f_p , however, was obtained from the nonzero calibration voltages because f_p was the same for a particular frequency whether the input voltage was 0.4, 0.8, 1.2, or 1.6 Vpp.

With these 6 additional points, a total of 30 calibration points were gathered. In retrospect, one or two more frequencies between 20 and 24 kHz should also have been added to identify where the filter transition region actually began.

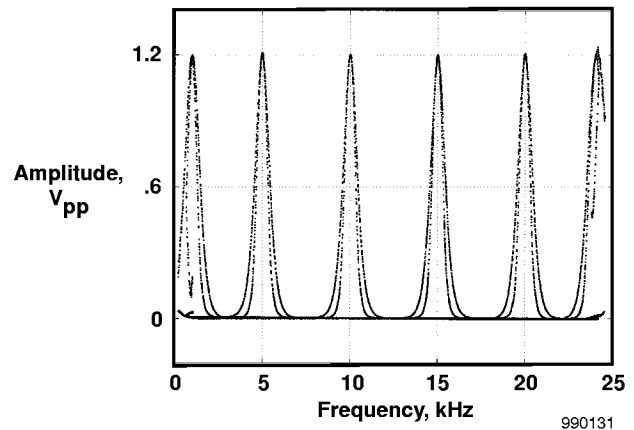
The calibration coefficients were calculated using the method of least-squares (ref. 14). The appendix shows the method applied to the amplitude calibration coefficients. The curve fit errors are ± 0.6 percent full scale for the amplitude and ± 0.1 percent full scale for the frequency.

Figure 5(a) shows superimposed uncalibrated readings obtained from one analysis channel and the sweep voltage channel given six of the calibration sine waves. Each frequency has two peaks because of the propagation delay discussed and illustrated in figure 4. The unequal heights of the spectra are evidence of the frequency-dependent gain discussed earlier.

Figure 5(b) is the result of applying calibration equations 2 and 6 with appropriate coefficients to the data in figure 5(a). The calibration equalizes the amplitudes and centers the spectra. For this figure, sweep direction was determined by comparing the value of one frequency reading with the value of the previous frequency reading. This scheme works adequately for most of the spectrum. At the extremes of the spectrum, however, the readings appear to belong to one sweep direction when, because of propagation delays, they really belong to the other. This fact explains why some of the results at 1 and 24 kHz appear incorrect.



(a) Uncalibrated readings. (Number in parentheses is the frequency in kHz.)



(b) Calibrated results.

Figure 5. Spectra for 1.2 Vpp sine waves at six frequencies.

FLIGHT DATA

On the FX-A experiment, the analyzer processed accelerometer data. The objective was to characterize vehicle vibration because, if the vibration level was too high at certain frequencies, subsequent boundary-layer experiments would not be worth performing.

In figure 6, two vibration spectra are superimposed. The dashed line represents the vibration level during captive carry flight, that is, before the rocket engine was ignited; the solid line represents the vibration level 19 sec after launch at high angle of attack.

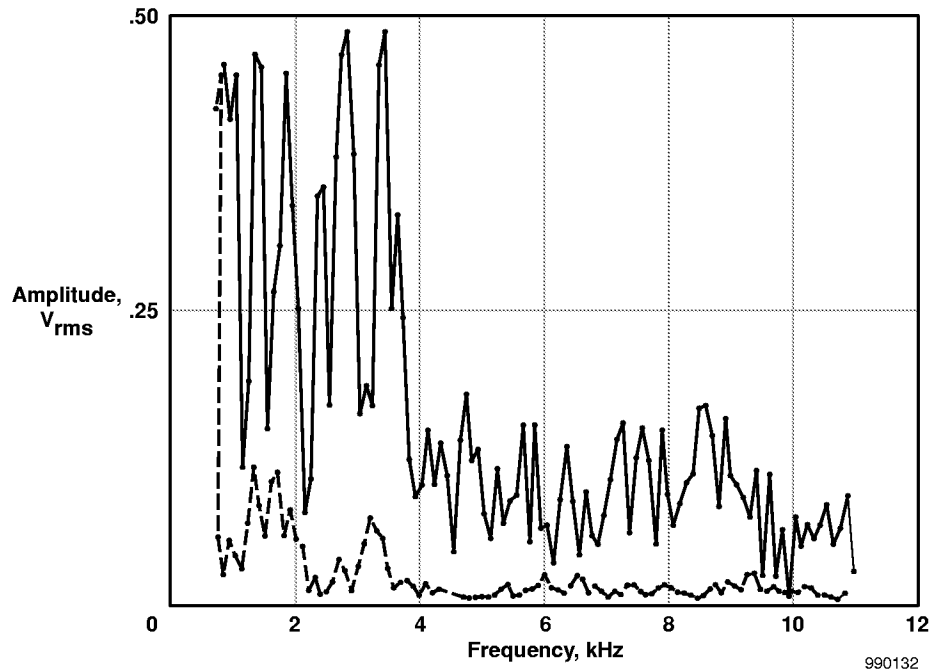


Figure 6. Accelerometer spectra before and after rocket ignition.

Each spectrum comes from one sweep, and the points are 100 Hz apart. Clearly the vibration level is higher after the rocket has been ignited than before. The vibration level drops off above 4 kHz—safely below the frequencies of interest for the FX-1 hypersonic boundary-layer transition experiment.

SUMMARY

This paper described the design and calibration of an airborne multichannel swept-tuned spectrum analyzer for characterization of dynamic data up to 25 kHz. The need for the analyzer was driven primarily by telemetry bandwidth limitations. After the data are transformed on board into the frequency domain, frequency resolution can be traded for reduced telemetry bandwidth. In the example presented, a factor of 6.25 in frequency resolution was sacrificed to reduce telemetry bandwidth by a factor of 10.

The analyzer design was based upon the widely used superheterodyne technique, and the frequency range of interest made the use of commercially available analog function modules possible. A four-channel analyzer was constructed in a small, lightweight, low-power package suitable for flight aboard the Pegasus® launch vehicle. The main limitation of the design was that the frequency content of the input signal remain stationary when the analyzer sweeps across the spectrum. Propagation delays in the analyzer were shown to require a set of calibration coefficients for each sweep direction. Frequency-dependent

coefficients were used for the amplitude calibration to deal with the sloped passband of the wideband input filter.

Finally, FX-A flight data illustrate how the spectrum analyzer is used, and gave confidence to proceed with FX-1.

REFERENCES

1. Bertelrud, Arild, et al., "Pegasus Wing-Glove Experiment to Document Crossflow Transition—Development and Current Status," AIAA-98-1522, 8th AIAA International Space Planes and Hypersonic Systems and Technologies Conference, Norfolk, Virginia, April 1998.
2. Graves, Sharon, et al., "High Frequency Data Acquisition Using Digital Signal Processing," AIAA-94-2134, 7th Biennial AIAA Flight Test Conference, Colorado Springs, Colorado, June 1994.
3. Bertelrud, Arild, et al., "Development of a System for Transition Characterization," AIAA-93-3465-CP, 11th AIAA Applied Aerodynamics Conference, Monterey, California, August 1993.
4. Diamond, John K., "Miniature PCM Compatible Wideband Spectral Analyzer for Hypersonic Flight Research," ISA-88-0732, Instrumentation Society of America 34th International Instrumentation Symposium, Albuquerque, New Mexico, May 1988.
5. Brown, Christie, "Spectrum Analysis Basics," 1997 Back to Basics Seminar, Hewlett-Packard Company, Santa Rosa, California, 1997, (HP Publication Number 5965-7008E).
6. Horowitz, Paul, and Winfield Hill, The Art of Electronics, Second Edition, Cambridge University Press, New York, New York, 1989: (a) "Measurements & Signal Processing," pp. 1035–1038; (b) "High Frequency & High-Speed Techniques," p. 890; (c) "Active Filters and Oscillators," pp. 273–276.
7. "Internally Trimmed Precision IC Multiplier: AD534," Special Linear Reference Manual, Analog Devices, Inc., Norwood, Massachusetts, 1992, pp. 2-15 to 2-22.
8. "4th- and 8th-Order Continuous-Time Active Filters: MAX274/MAX275," 1993 New Releases Data Book, Volume II, Maxim Integrated Products, Sunnyvale, California, 1993, pp. 6-3 to 6-29.
9. "High Precision, Wideband RMS-to-DC Converter: AD637," Special Linear Reference Manual, Analog Devices, Inc., Norwood, Massachusetts, 1992, pp. 4-23 to 4-30.
10. Lancaster, Don, revised by Howard M. Berlin, "Counters and Shift Registers," CMOS Cookbook, Second Edition, Howard W. Sams & Co., Indianapolis, Indiana, 1988, pp. 379–383.
11. "Voltage-to-Frequency and Frequency-to-Voltage Converter: AD650," Data Converter Reference Manual, Volume II, Analog Devices, Inc., Norwood, Massachusetts, 1992, pp. 3-15 to 3-26.
12. "Dual Current Source/Current Sink: REF200," Burr-Brown IC Data Book—Linear Products, Burr-Brown Corporation, Tucson, Arizona, 1995, p. 8.59 (figure 12, "Precision Triangle Wave Form Generator").

13. Ludeman, Lonnie C., “The Discrete Fourier Transform,” Fundamentals of Digital Signal Processing, John Wiley & Sons, New York, New York, 1986, p. 287.
14. Dally, James W., et al., “Statistical Methods in Experimental Measures,” Instrumentation for Engineering Measurements, John Wiley & Sons, Inc., New York, New York, 1984, pp. 534–539.
15. Strang, Gilbert, “Orthogonal Projections and Least Squares,” Linear Algebra and Its Applications, Second Edition, Academic Press, New York, New York, 1980, p. 138.
16. “Matrices and Linear Algebra,” Using MATLAB, The MathWorks, Inc., Natick, Massachusetts, December 1996, pp. 4-13, 4-22, and 4-23.

APPENDIX—SOLVING FOR THE CALIBRATION COEFFICIENTS

Using subscripts 1 through 30 to denote the 30 calibration points, 30 equations in the form of equation 6 are obtained. The key to solving for the set of coefficients that has minimum error in the least-squares sense is to organize the terms of the equations into vectors and a matrix; namely,

$$\begin{bmatrix} V_1 \\ \cdot \\ \cdot \\ \cdot \\ \cdot \\ V_{30} \end{bmatrix} = \begin{bmatrix} 1 & f_{p_1}^{-1} & f_{p_1} & f_{p_1}^2 & f_{p_1}^3 & v_{p_1} & v_{p_1} f_{p_1}^{-1} & v_{p_1} f_{p_1}^{-2} & v_{p_1} f_{p_1} & v_{p_1} f_{p_1}^2 \\ \cdot & \cdot & \cdot & \cdot & \cdot & \cdot & \cdot & \cdot & \cdot & \cdot \\ \cdot & \cdot & \cdot & \cdot & \cdot & \cdot & \cdot & \cdot & \cdot & \cdot \\ \cdot & \cdot & \cdot & \cdot & \cdot & \cdot & \cdot & \cdot & \cdot & \cdot \\ \cdot & \cdot & \cdot & \cdot & \cdot & \cdot & \cdot & \cdot & \cdot & \cdot \\ 1 & f_{p_{30}}^{-1} & f_{p_{30}} & f_{p_{30}}^2 & f_{p_{30}}^3 & v_{p_{30}} & v_{p_{30}} f_{p_{30}}^{-1} & v_{p_{30}} f_{p_{30}}^{-2} & v_{p_{30}} f_{p_{30}} & v_{p_{30}} f_{p_{30}}^2 \end{bmatrix} \begin{bmatrix} c_0 \\ \cdot \\ c_4 \\ b_0 \\ \cdot \\ b_4 \end{bmatrix}$$

If vector V_1 through V_{30} is represented by \mathbf{b} , vector $[c_0..c_4b_0..b_4]$ by \mathbf{x} , and the matrix by \mathbf{A} , then the system of equations is in the form of $\mathbf{Ax} = \mathbf{b}$. This structure is common in linear algebra and has a standard solution; namely, $\mathbf{x} = (\mathbf{A}^T \mathbf{A})^{-1} \mathbf{A}^T \mathbf{b}$, where \mathbf{A}^T is the transpose of \mathbf{A} and $(\mathbf{A}^T \mathbf{A})^{-1} \mathbf{A}^T$ is the pseudoinverse of \mathbf{A} (ref. 15). The solution looks complicated, but mathematics software packages that handle matrices (ref. 16) are commercially available to compute the solution.

